Electronic Supplementary Material (ESI) for Dalton Transactions

Electronic Supplementary Information

pH-controlled assembly of hybrid architectures based on Anderson-type polyoxometalates and silver coordination units

Ying Hu,[a] Haiyan An,*[a] Xuan Liu,[a] Jiqiu Yin,*[b] Huilong Wang,[a] Hua Zhang,[a] Lin Wang[a]

[a]*College of Chemistry, Dalian University of Technology, Dalian 116023, P. R. China*

[b]*College of Medical Laboratory, Dalian Medical University, Dalian 116044, P. R. China*

Table S1 Selected bond lengths (Å) and angles (˚) for **1**–**3**.

Compound **1**[a]			
Mo(1)-O(8)	1.701(5)	Mo(1)-O(5)	1.901(4)
Mo(1)-O(7)	1.717(4)	Mo(1)-O(4)	1.951(4)
Mo(1)-O(2)	2.291(4)	Mo(2)-O(9)	1.712(4)
Mo(2)-O(2)	2.329(4)	Mo(3)-O(12)	1.725(4)
Al(1)-O(1)	1.901(4)	Al(1)-O(2)	1.889(4)
Al(1)-O(3)	1.913(4)	Ag(1)-O(7)#3	2.389(4)
Ag(2)-N(1)	2.098(5)	Ag(1)-O(9)	2.290(4)
O(1)-Al(1)-O(3)#1	85.05(16)	O(1)-Al(1)-O(3)	94.95(16)
O(2)#1-Al(1)-O(2)	180.0(2)	O(3)#1-Al(1)-O(3)	180.0(3)
Compound **2**[b]			
Mo(1)-O(7)	1.706(4)	Mo(2)-O(10)	1.709(4)
Mo(1)-O(5)	1.948(3)	Mo(2)-O(9)	1.721(4)
Mo(1)-O(1)	2.287(3)	Mo(2)-O(5)	1.911(4)
Mo(1)-O(2)	2.322(3)	Mo(3)-O(12)	1.710(4)
Ag(1)-N(2)	2.160(4)	Mo(3)-O(11)	1.711(4)
Ag(1)-N(1)	2.162(4)	Ag(1)-O(11)	1.875(3)
Al(1)-O(1)	1.875(3)	Al(1)-O(3)	1.923(3)
Na(1)-O(12)#1	2.584(5)	Na(1)-O(14)#4	2.526(5)
Na(1)-O(7)	2.372(5)		
O(2)-Al(1)-O(3)	85.00(13)	O(1)-Al(1)-O(3)	95.07(13)
O(2)-Al(1)-O(2)#1	180.00(12)	O(3)-Al(1)-O(3)#1	180.00(15)
Compound **3**[c]			
Mo(1)-O(7)	1.714(3)	Mo(1)-O(1)	2.241(2)
Mo(1)-O(8)	1.722(3)	Mo(1)-O(2)	2.337(2)
Mo(2)-O(9)	1.708(3)	Mo(2)-O(6)	1.910(2)
Mo(2)-O(10)	1.725(3)	Mo(3)-O(4)#1	1.954(2)
Mo(3)-O(11)	1.702(3)	Mo(3)-O(12)#1	1.720(3)
Al(1)-O(1)	1.885(2)	Al(1)-O(2)	1.903(2)
Al(1)-O(3)	1.914(2)	Ag(1)-O(10)	2.429(3)
Ag(1)-O(8)#2	2.314(3)	Ag(1)-O(9)#2	2.557(3)
Ag(1)-OW1	2.267(3)	Ag(1)-OW2	2.639(3)
Ag(2)-O(12)	2.447(3)	Ag(2)-O(7)	2.374(3)
Ag(2)-O(13)	2.741(3)		
O(1)-Al(1)-O(3)#1	84.37(10)	O(1)#1-Al(1)-O(3)#1	95.63(10)
O(1)-Al(1)-O(1)#1	180.0	O(3)#1-Al(1)-O(3)	180.0

[a] Symmetry transformations used to generate equivalent atoms: #1 -x,-y,-z #3 -x-1/4,-y-1/4,z

[b] Symmetry transformations used to generate equivalent atoms: #1 -x+2,-y,-z+1 #4 -x+2,y+1/2,-z+3/2

[c] Symmetry transformations used to generate equivalent atoms: #1 -x-1,-y+2,-z+1 #2 -x,-y+1,-z+1

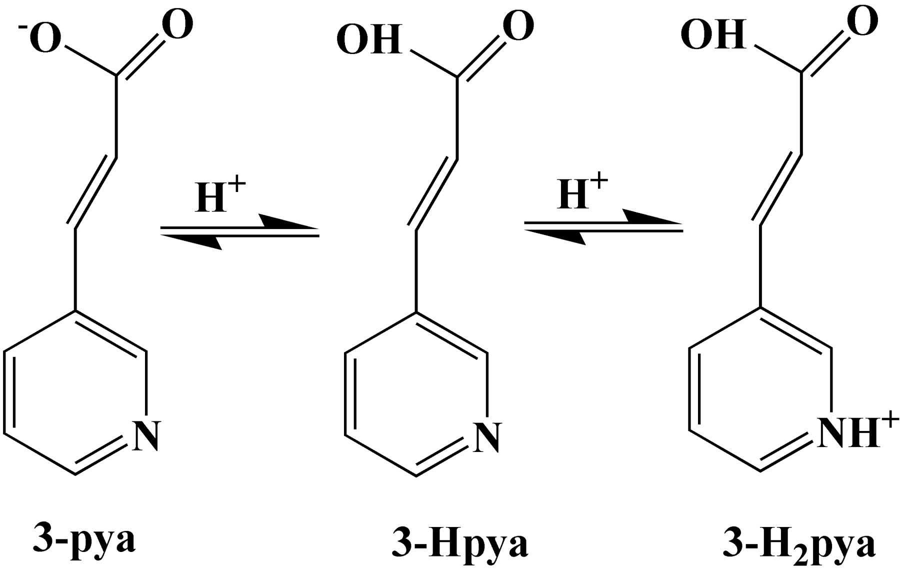

Scheme S1 Scheme showing ligand notation.

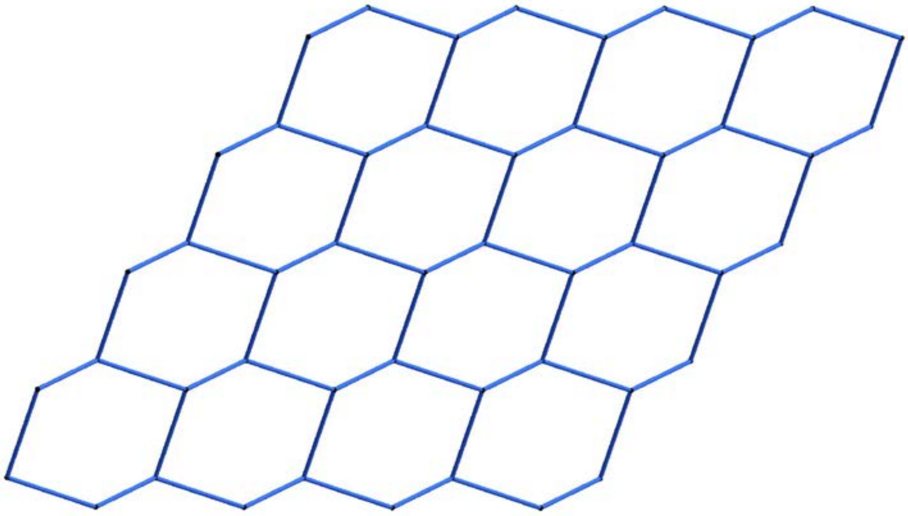

Fig. S1 Schematic representation of the 2D layer in **1**.

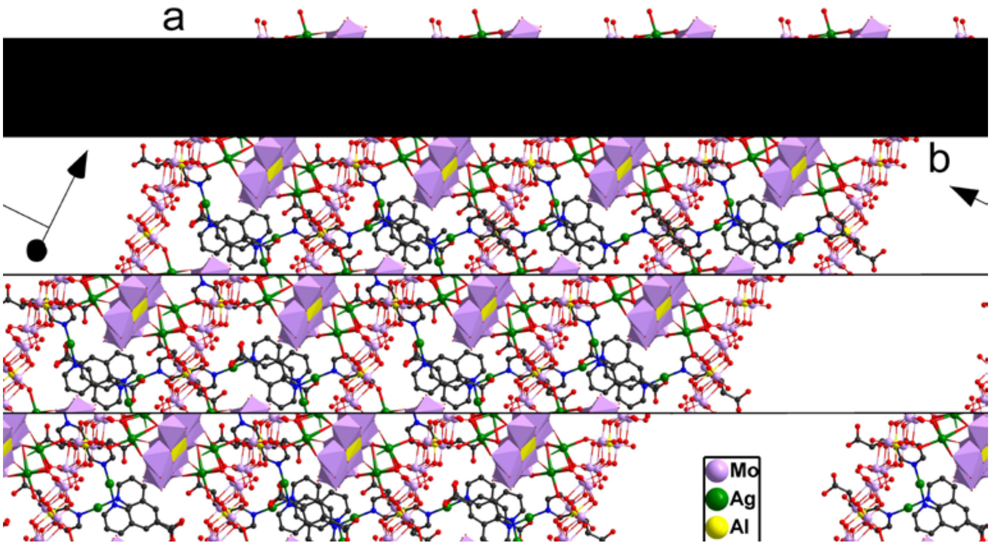

[redacted]

Fig. S2 Polyhedral and ball-stick view of the 3D host-guest framework in **1** with Ag-3-Hpya coordination complexes as template (color code: Al, yellow; Mo, pink; Ag, green; O, red; N, blue; C, grey).

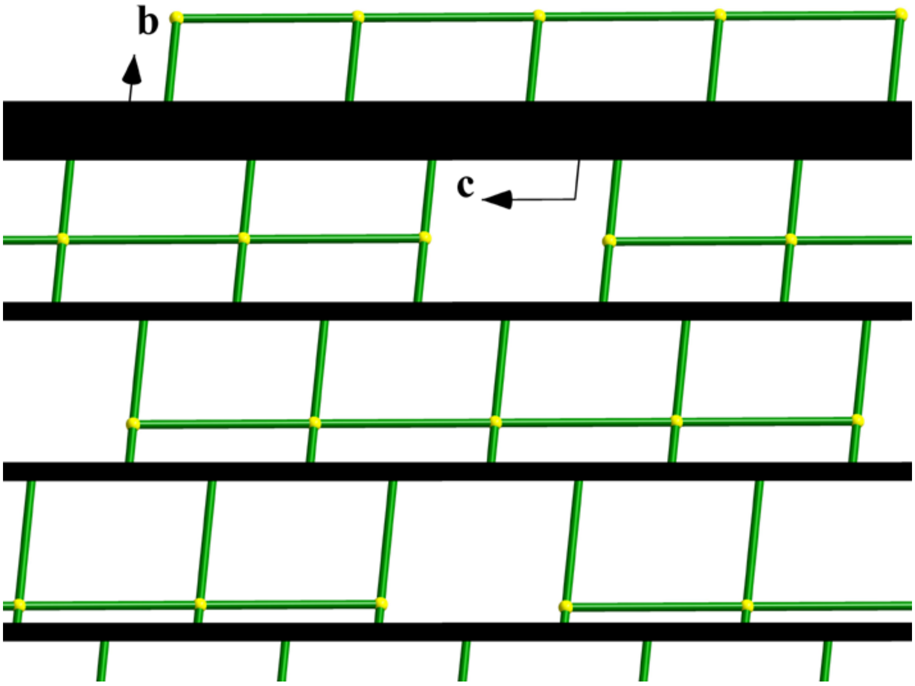

[redacted]

[redacted]

[redacted]

[redacted]

Fig. S3 Schematic representation of the 4^4 topology of **3**.

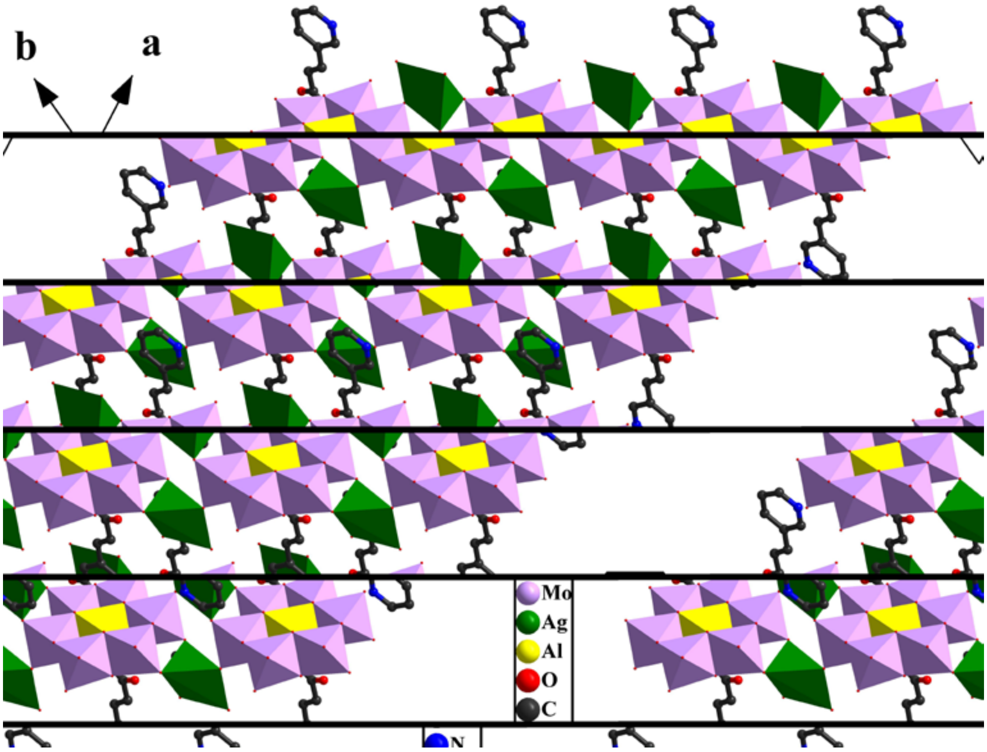

Fig. S4 Polyhedral and ball-stick view illustrating the 3D supramolecular structure of **3** along the *c* axis (color code: Al, yellow; Mo, pink; Ag, green; O, red; N, blue; C, grey).

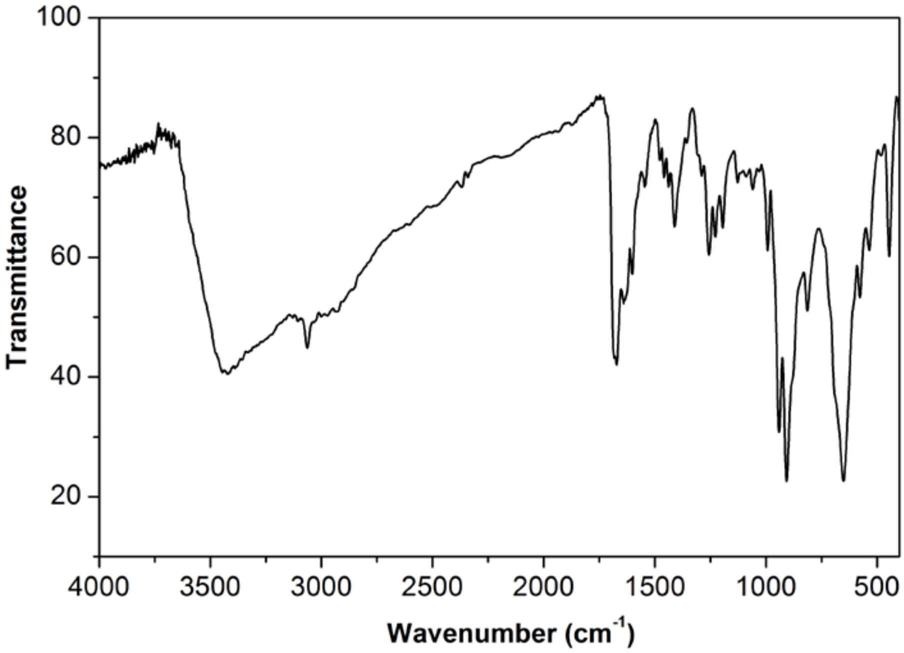

Fig. S5a IR spectrum for compound **1**.

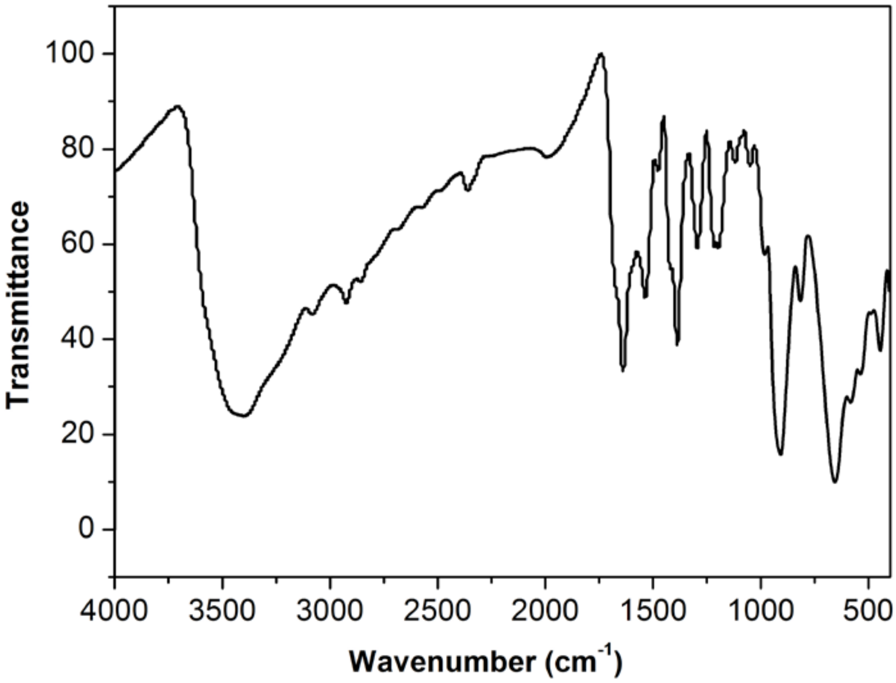

Fig. S5b IR spectrum for compound **2**.

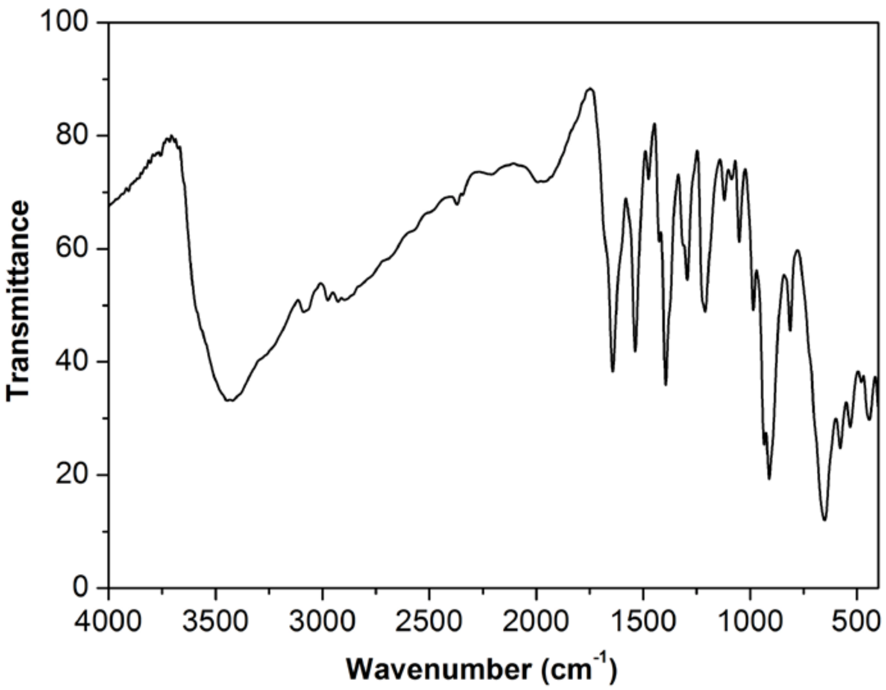

Fig. S5c IR spectrum for compound **3**.

FT-IR spectroscopy

IR spectra of compounds **1–3** display similar characteristic patterns of the Anderson-type structure $[AlMo_6H_6O_{24}]^{3-}$ with vibration bands between 900 and 950 cm^{-1} for the Mo–Ot units, between 640 and 700 cm^{-1} for the Mo–Ob groups, and between 400 and 600 cm^{-1} for the Mo–Oc bonds. In the IR spectrum of compound **1**, the features at 1672 and 1412 cm^{-1} can be regarded as characteristics of the 3-Hpya molecule. The features at 1639 and 1389 cm^{-1} in compound **2** can be regarded as characteristics of the 3-Hpya molecule. In the IR spectrum of compound **3**, the features at 1642 and 1395 cm^{-1} can also be regarded as characteristics of the 3-Hpya molecule. A broad band around 3420 cm^{-1} of **1**, 3402 cm^{-1} of **2** and 3421 cm^{-1} of **3** is attributed to the absorptions of water molecules.

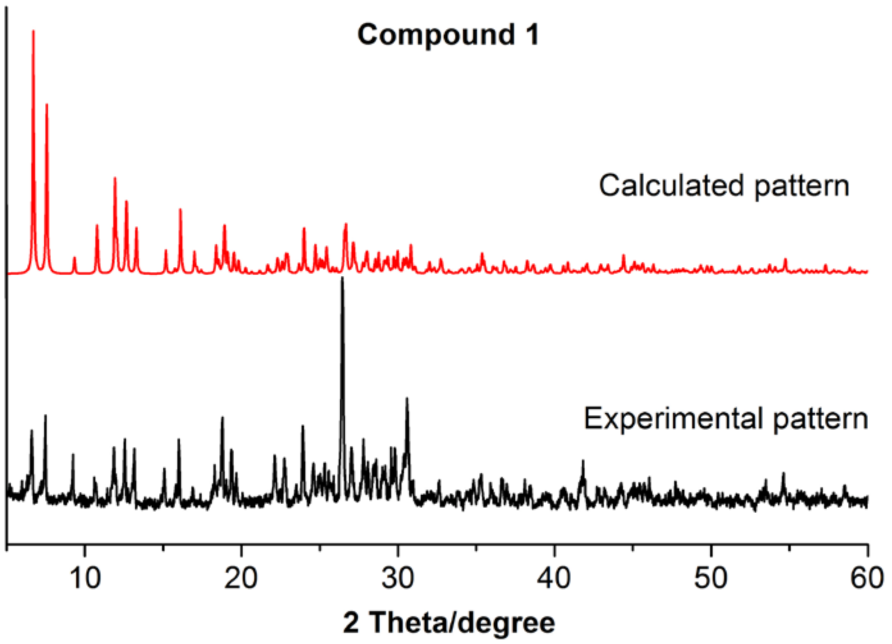

Fig. S6a The calculated and experimental PXRD patterns for compound **1**.

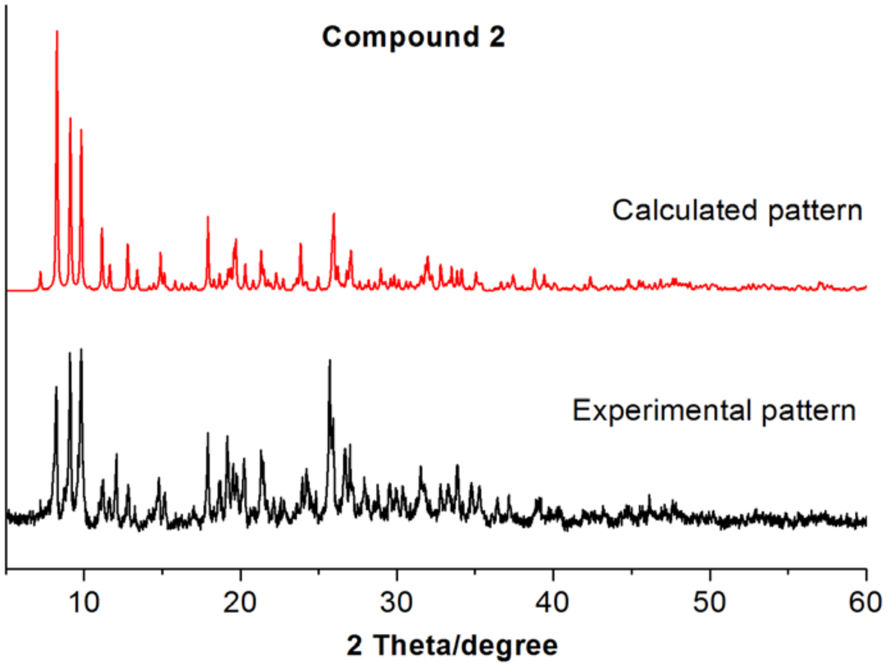

Fig. S6b The calculated and experimental PXRD patterns for compound **2**.

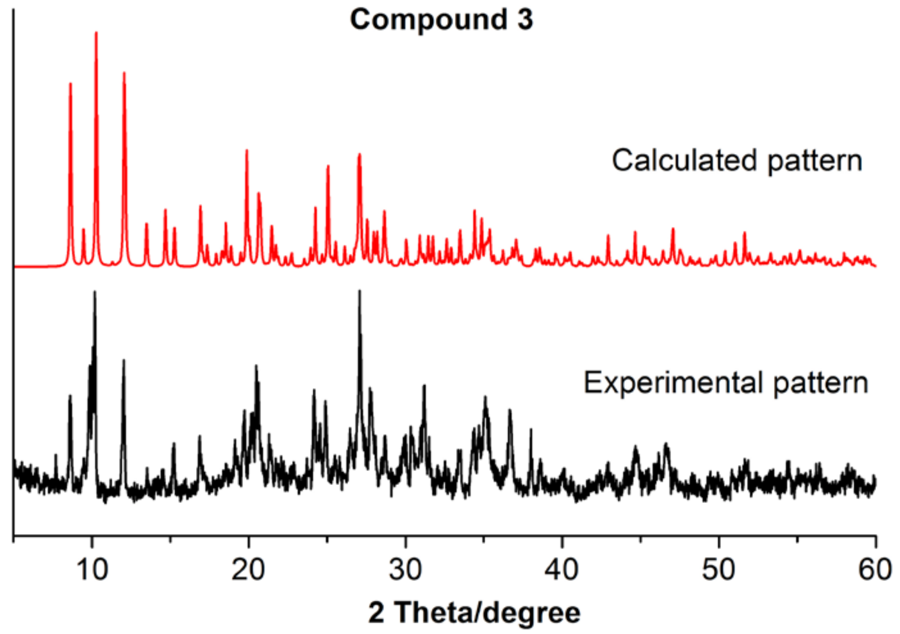

Fig. S6c The calculated and experimental PXRD patterns for compound **3**.

PXRD Characterization

The PXRD patterns for **1–3** are presented in Fig. S6. The diffraction peaks of both calculated and experimental patterns match well, indicating the phase purities of these compounds. The differences of PXRD patterns of **1–3** also indicate that three compounds have different structures. These conclusions are in agreement with the results of the single crystal X-ray analysis.

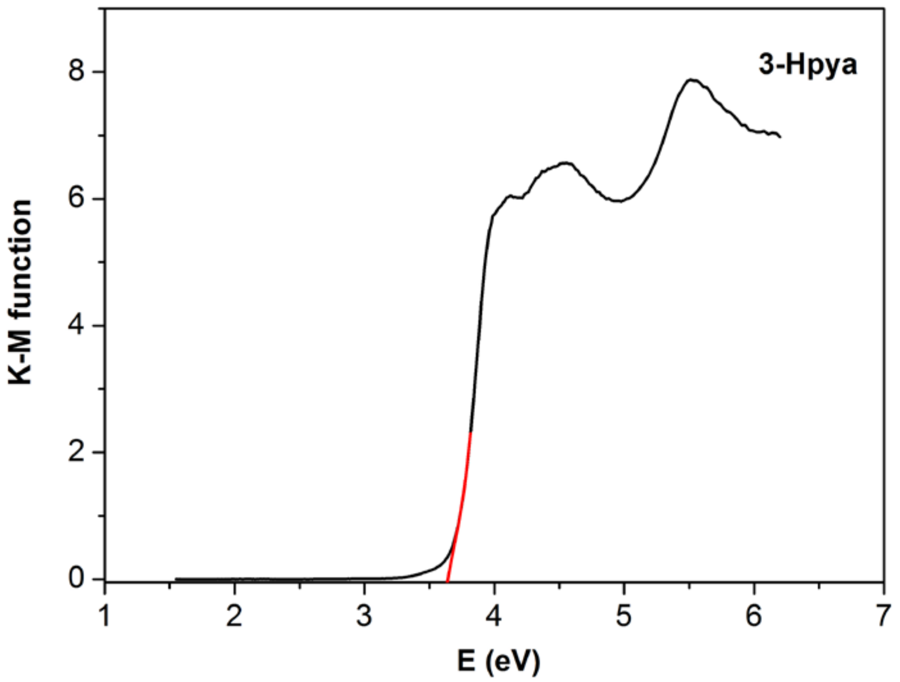

Fig. S7 UV−vis-NIR diffuse reflectance spectra of K−M functions vs energy (eV) of 3-Hpya ligand.

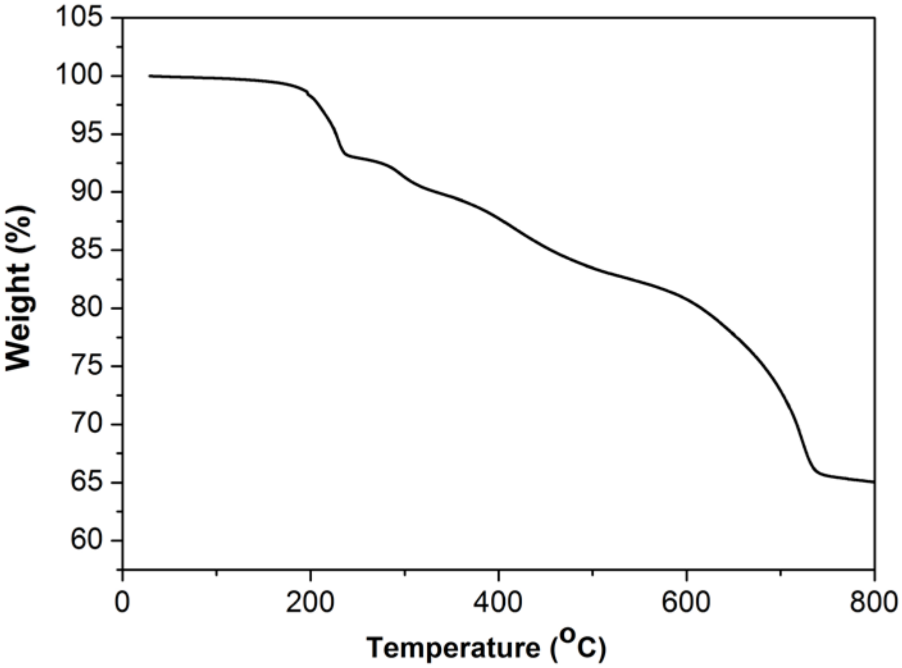

Fig. S8a The TG curve of **1** exhibits a multi-step continuous weight loss process and gives a total weight loss of 34.9% in the range of 30–800 ºC, which agrees with the calculated value of 33.9%. The weight loss of 7.1% at 70–250 ºC corresponds to the loss of all lattice and composition water molecules (calc. 6.8%). The weight loss of 27.8% at 255–790 ºC arises from the decomposition of 3-Hpya molecules, and partial oxygen molecules (calc. 27.1%).

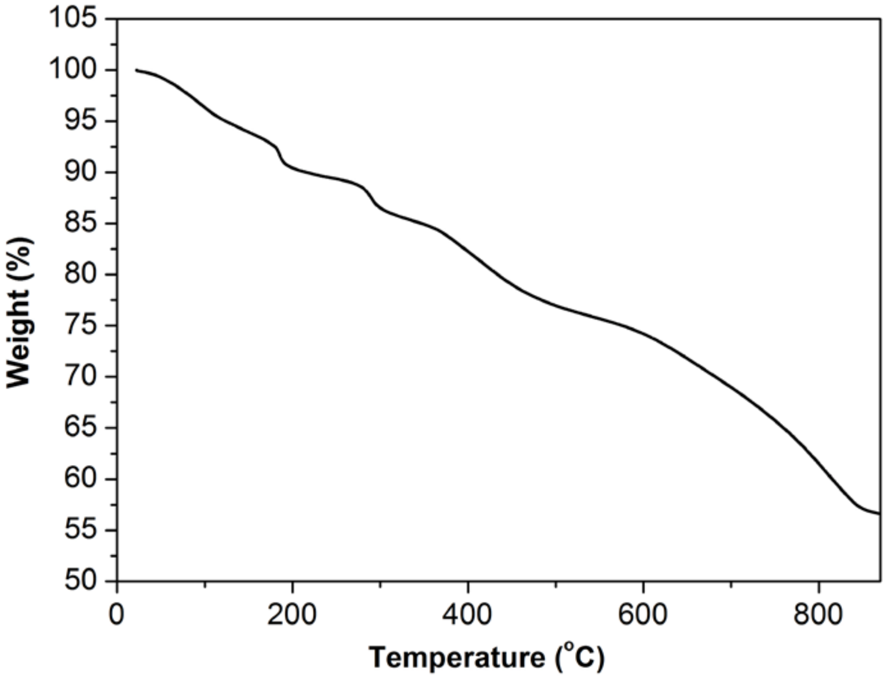

Fig. S8b TG curve of **2** exhibits a multi-step continuous weight loss process and gives a total weight loss of 43.4% in the range of 22–870 ºC (calc. 40.2%). The weight loss of 10.3% from 25 to 230 ºC corresponds to the loss of adsorbed water, all lattice and partial composition water molecules. The weight loss of 4.3% from 235 to 330 ºC is due to the loss of residual water molecules and partial 3-Hpya molecules. The weight loss of 28.8% from 333 to 870 ºC arises from the loss of 3-Hpya molecules, and partial oxygen molecules.

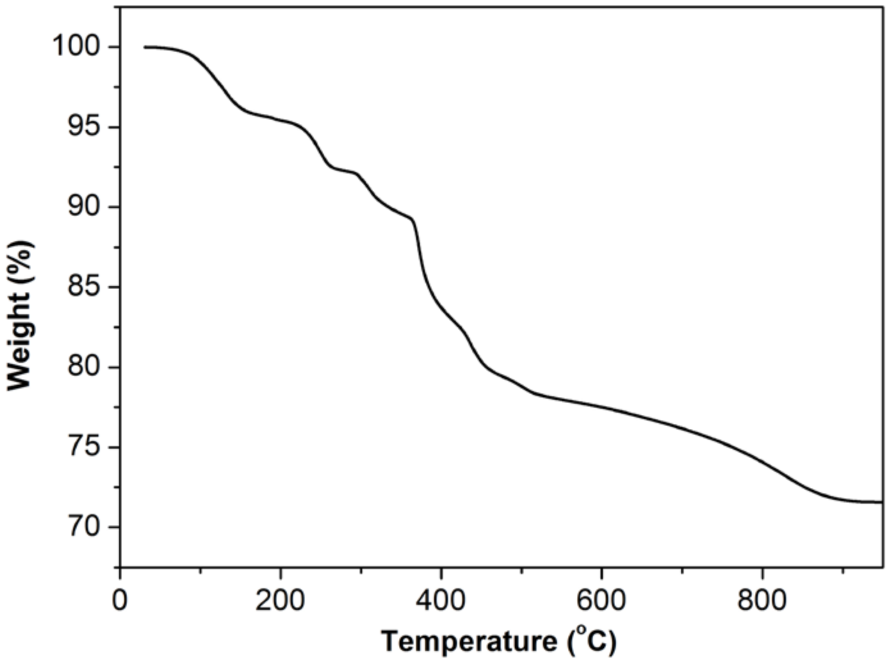

Fig. S8c TG curve of **3** also possesses a multi-step continuous weight loss process and gives a total loss of 28.5% in the range of 30–950 ºC (calc. 28.1%). The three-step continuous weight loss of 10.2% from 40 to 340 ºC arises from the loss of all lattice, coordinated and composition water molecules (calc. 9.4%). The continuous weight loss of 18.3% from 340 to 910 ºC is due to the loss of 3-Hpya molecules, and partial oxygen molecules.

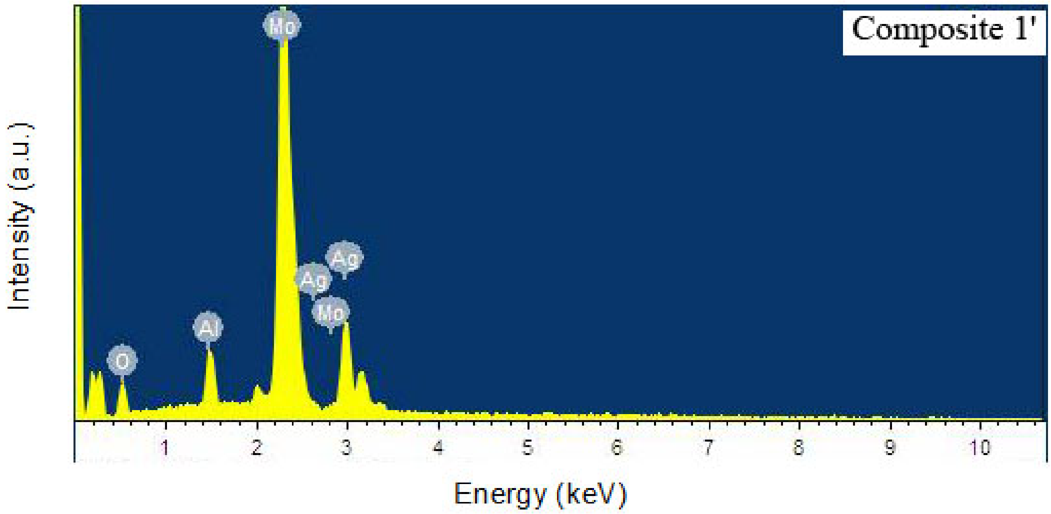

Fig. S9a Energy-dispersive X-ray (EDX) spectrum obtained from a typical sample of nanocomposite **1'** and showing the presence of silver, molybdenum, aluminum and oxygen. (The $C_{K\alpha}$ signal at 0.28 keV is due to the C substrate).

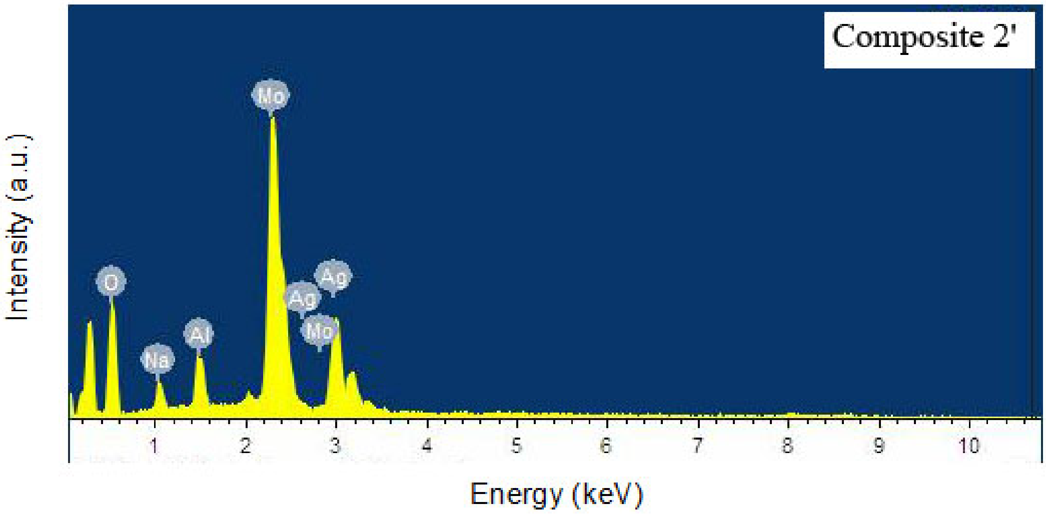

Fig. S9b Energy-dispersive X-ray (EDX) spectrum obtained from nanocomposite **2'** and showing the presence of silver, molybdenum, aluminum, sodium and oxygen. (The $C_{K\alpha}$ signal at 0.28 keV is due to the C substrate).

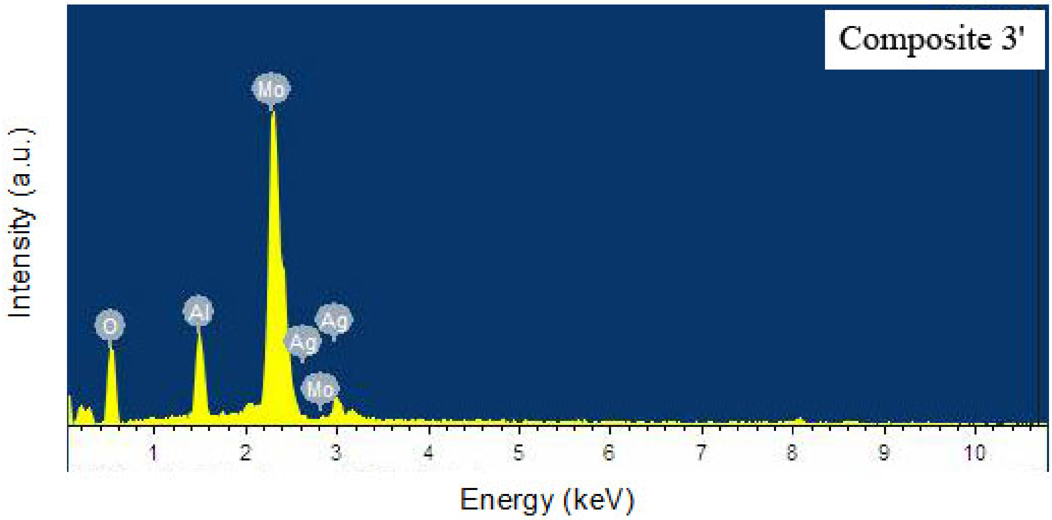

Fig. S9c Energy-dispersive X-ray (EDX) spectrum obtained from nanocomposite **3'** and showing the presence of silver, molybdenum, aluminum, and oxygen. (The $C_{K\alpha}$ signal at 0.28 keV is due to the C substrate).

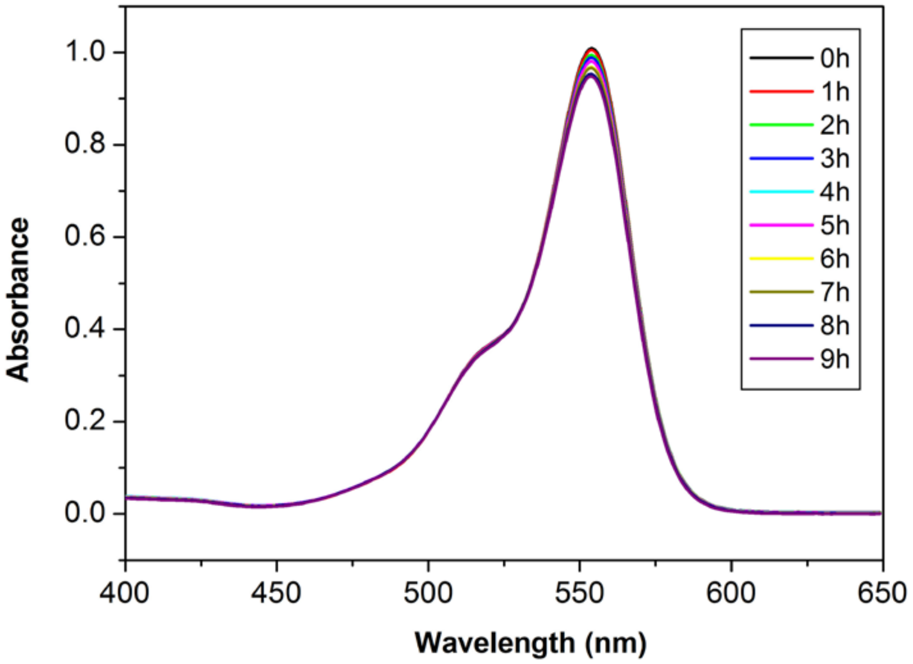

Fig. S10 UV–Vis spectral changes of RhB (2 x 10^{-5} M) in aqueous solution against time without catalyst.

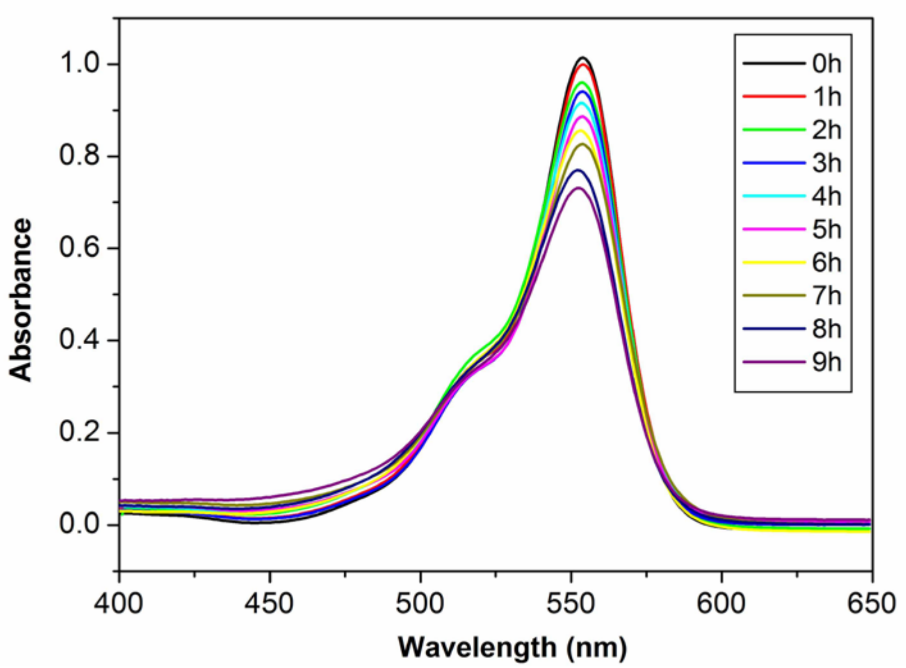

Fig. S11 UV–Vis spectral changes of RhB (2 x 10^{-5} M) in aqueous solution against time with the use of $(NH_4)_3[AlMo_6H_6O_{24}]$ as catalyst.

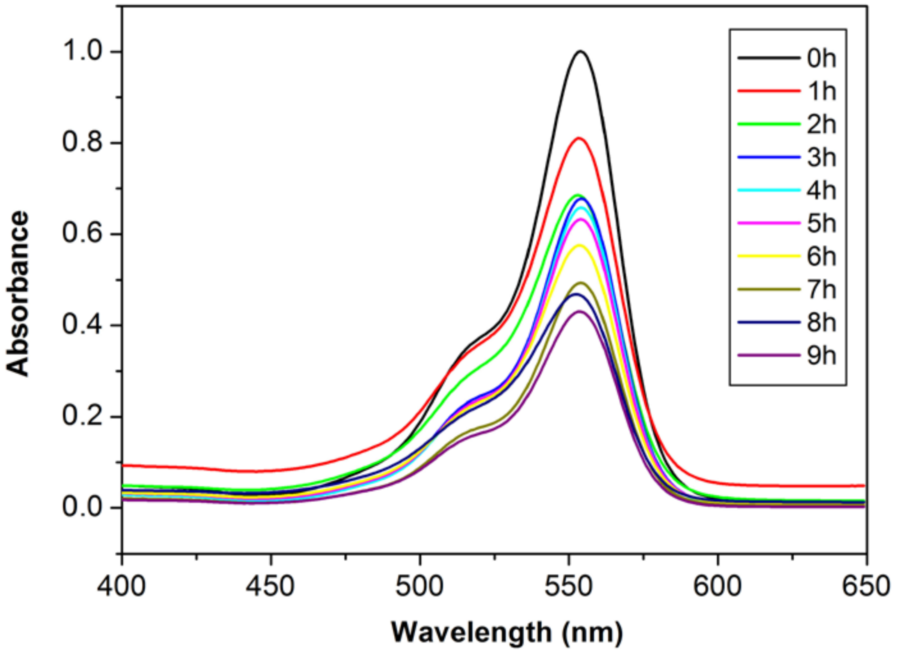

Fig. S12 UV–Vis spectral changes of RhB (2 x 10^{-5} M) in aqueous solution against time with the use of compound **1** as catalyst.

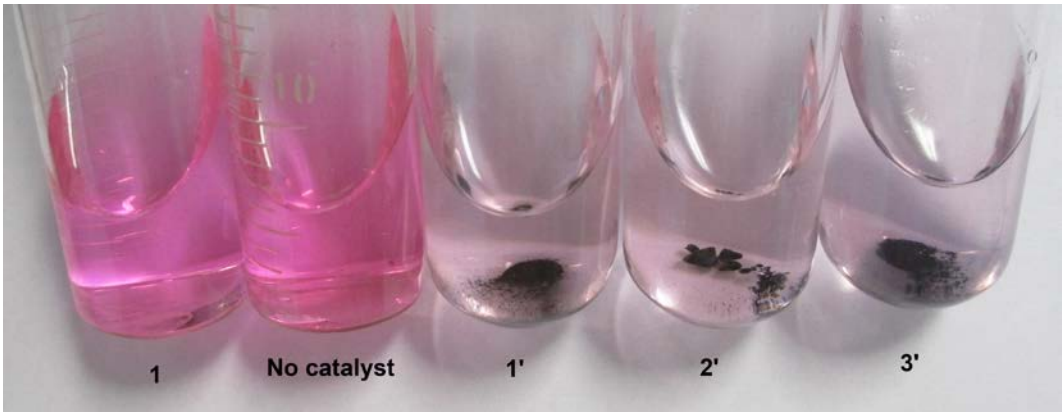

Fig. S13 The color of the RhB solution changes after 9h with catalysts **1**, **1'**, **2'**, **3'** and without catalyst.